Quaternary International xxx (2016) 1–15

Contents lists available at ScienceDirect

Quaternary International

journal homepage: www.elsevier.com/locate/quaint

Lacustrine clay mineral assemblages as a proxy for land-use and climate changes over the last 4 kyr: The Amik Lake case study, Southern Turkey

Meriam El Ouahabi [a, *], Aurélia Hubert-Ferrari [b], Nathalie Fagel [a]

[a] University of Liège, AGEs, Department of Geology, Liège, Belgium
[b] University of Liège, Department of Geography, Liège, Belgium

ARTICLE INFO

Article history:
Received 17 June 2016
Received in revised form
18 November 2016
Accepted 23 November 2016
Available online xxx

Keywords:
Soil
Weathering conditions
Land erosion
Clay mineralogy
Lake sediments
Last millennia

ABSTRACT

Lake sediments are sensitive to landscape changes and most of these changes seem to be modulated by land-use (anthropogenic factors) coupled to palaeoenvironmental/palaeoclimatic changes. In its detrital fraction, the lacustrine sediments record the history of soil erosion within its catchment via the inputs of clays and others detrital products. Within a Mediterranean context, the study investigates the upper sediments infilling the central part of the Amik basin in southern Turkey. This tectonic basin was occupied and exploited by modern human at least since 6000–7000 BCE. We focus on the clay mineralogy (x-ray diffraction on oriented aggregates) and magnetic susceptibility measurements (Bartington) of the sedimentary record in the area over the last 4000 years, to assess environmental changes in relation with the different land uses and/or weathering during the successive Bronze, Iron, Roman, Islamic/Ottoman and Modern civilizations. The clay fraction of Amik Lake sediments comprises smectite, kaolinite, illite, chlorite and chlorite/smectite mixed layers that are the inherited clay phases. A relative change in abundance and crystallinity and chemistry of illite attests that environmental conditions evolved in the Amik Plain from the Bronze to Modern Age in relation with climates and/or land-use changes. The history of the Amik Lake reveals different soil erosion episode. The most intense erosion phase occurred during the Bronze/Iron Ages as indicated by the clay and magnetic susceptibility proxies. The Roman period was an exceptional period with soil erosion products arriving from the watershed, probably due the water channelization. A reduction of soil erosion occurred during the post Roman period until nowadays. Significant pedogenesis transformations are evidenced, especially during the Islamic/Ottoman periods suggesting intense chemical weathering conditions related to climate change.

1. Introduction

Soil-forming environments and erosion processes are strongly influenced by land-use practices which changed through human history in a given area (e.g. Lawrence et al., 2015). Other influencing factors, such as permanent parameters (seismology, lithology, relief), and variable factors (climate, hydrology, vegetation cover) have also an impact on sediment yield and erosion rates (e.g. Edwards and Whittington, 2001; Lucke et al., 2005; Dodson et al., 2004; Pelle et al., 2013; Vogel et al., 2016). These natural and anthropogenic factors are difficult to untangle (Berglund, 2003; Ackermann et al., 2014). Indeed, soil erosion can be induced by climate changes (strong precipitations, seasonality and aridity) as well as more intense land-use (Pécsi, 1990; Günster and Skowronek, 2001; Casana, 2008; Zielhofer et al., 2008; Jalut et al., 2009; Varga et al., 2011; Costantini et al., 2012; Sauer et al., 2015).

This problematic is particularly acute in the Amik Plain area (also known as the Plain of Antioch) in the southern Turkey, which has a long history of dense human settlement dating back at least to the Pottery Neolithic (7000 BCE) (Braidwood and Braidwood, 1960). Numerous studies were undertaken in the region in order to reconstruct the environmental and settlements history through an interdisciplinary regional research program, incorporating archaeological settlement survey, geomorphological and paleoenvironmental analyzes, and targeted excavations at key sites of various periods (Braidwood and Braidwood, 1960; Yener et al., 2000; Yener and Batiuk, 2010; Lawrence et al., 2015). A first major settlement phase occurred during the Bronze-Iron Ages, 3000–500 BCE (Wilkinson, 2000; Casana, 2007). The lands around

* Corresponding author.

http://dx.doi.org/10.1016/j.quaint.2016.11.032
1040-6182/

tells and on low-dipping reliefs were used for wheat culture and orchards (Wilkinson, 2000; Casana, 2007). A second settlement phase more intensive occurred during the Hellenistic, Roman and Late Roman periods (300 BC-650 AD), and was associated with the conversion of upland areas for an intensive agricultural production (Wilkinson, 1997, 2000). This change was linked to the birth and growth of the city of Antioch, one of the largest city in the Roman Empire, with may be up to 500 000 inhabitants including its suburbs. During the Late Roman period, the Amik Plain was more densely occupied than at any time in its history (Casana, 2008). Agricultural farming associated with an irrigation network was developed around the city of Antioch and in the Amik Basin in order to feed its large population. Around 700–900 AD, numerous Roman sites were progressively abandoned in the basin and in the highlands (Casana, 2007).

The spatial and temporal extent and organisation of the settlements in the Amik Plain are well constrained but not its possible impact on the environment (Yener et al., 2000; Wilkinson et al., 2001). In the present paper we propose to consider this issue by characterizing soil erosion in the Amik Plain using clay mineralogy and magnetic susceptibility as proxy indicators. An overview of the climatic conditions that prevailed in this area is also the main objective. To achieve this, 6 m long sedimentary record was analyzed to define the clay types deposited in the plain and their weathering characteristics. Clay mineralogy is then used to try to untangle soil erosion, land-use and climate change in this critical zone.

2. Regional, tectonic and geological setting

The Amik Plain is situated in the Eastern Mediterranean basin within the borders of the Hatay province. It is surrounded by several mountain ranges and plateaus. To the west part, the Amanus Mountain culminating at 2250 m, is an ophiolitic complex and its sedimentary cover (Boulton et al., 2007). To the south, lie the low ranges of calcareous Jebel al-Aqra or Kuseyr Plateau. To the northeast, the Kurt Mountains culminating at 825 m are mainly composed of metamorphic rocks (Wilkinson, 2000; Robertson, 2002; Altunel et al., 2009; Parlak et al., 2009; Eger, 2011; Karabacak and Altunel, 2013). The ~50 km long and 50 km wide basin itself is filled with up to 2.5 km thick Plio-Quaternary sediments (Gülen et al., 1987), and is crossed by the left-lateral Dead Sea Fault (DSF), which is active and ruptured during the large destructive earthquakes (Akyuz et al., 2006; Altunel et al., 2009; Karabacak et al., 2010; Karabacak and Altunel, 2013). The Basin was temporally occupied by the Amik Lake.

The Amik lake has a complex history with alternating extension and disappearance (Friedman et al., 1997; Wilkinson, 1997, 2000; Casana, 2008). During the Roman period, the Afrin and the Karasu rivers draining into the Amik Lake were partly channelized, starting probably around 50 AD; some channels were used at least until the early Islamic period (~700 AD) (Wilkinson and Rayne, 2010). The lake started to be artificially drained in the 1940's for the cultivation of cotton and to eradicate malaria (Çalışkan, 2008), but its wetland were still covering a large area. A more intense desiccation work started in the 1966 and by 1972 the three rivers draining into the basin were channelized. The lake and its wetland were completely destroyed in 1987 (Kilic et al., 2006). As results, the cropland area increased by 174% (Kilic et al., 2006).

3. Material and methods

3.1. Coring site

The site (N 36°20.655'– E 036°20°.948') is located just at the border of the Kumtepe village, near the former eastern border of the Amik Lake defined by a low sandy ridge containing Roman pottery and lacustrine shells (Yener et al., 2000). In this area the major water inflow is provided by the Afrin River (Fig. 1). In addition the site stands near the DSF fault (Karabacak et al., 2010) and is adjacent to the following archaeological sites: Tell Kara Tepe (AS86) and Kurdu which are Bronze and Early-Middle Chalcolithic sites, respectively (Yener et al., 2000). It also lies near a Roman canal draining the water from the Afrin River, which cessed to be used after the 2nd century CE (Casana, 2012).

Sediments were collected in a trench every 1 cm during the summer time, July 1st, 2012. At this period the water table was 1.5 m deep. The sampling was extended to 6 m depth thanks to a drill core.

3.2. Methods

3.2.1. Magnetic susceptibility and X-ray diffraction studies

Magnetic susceptibility (MS) performed every 1 cm using MS2 magnetic susceptibility system. Magnetic susceptibility was used as a first indicator of input of terrigenous materials, allochthonous to the lake (Hubert-Ferrari et al., 2012).

Mineralogical and geochemical analyzes were performed at 5 cm resolution to highlight the occurrence of environmental changes. Furthermore, clay mineralogy was carried out at lower resolution (10–20 cm) depending mainly on the changes in chemical and mineralogical composition. In particular, sample selection for clay mineralogy analysis was based on the peaks shape on the bulk XRD diffractogram at (001) reflections and the possible presence of the mixed layers clays mineral (10–14 A°).

The clay mineralogical analysis was performed by X-ray diffraction (XRD), using a Bruker D8 ADVANCE diffractometer, equipped with a Cu-$K\alpha$ radiation on the <2 μm fraction (Universality of Liège, Belgium). For the clay fraction analysis the whole sediment was decarbonated with HCl (0.1 mol/L) and the <2 μm fraction separated by settling in a water column. Samples were mounted as oriented aggregates on glass slides (Moore and Reynolds, 1997). For each sample three X-ray patterns were recorded: air-dried (N), ethylene-glycol solvated for 24 h (EG), and heated at 500 °C for 4 h (H).

The background noise of the X-ray patterns was removed and profile parameters such as line positions, Full Width at Half Height Width (FWHM), peak intensities were calculated by the *DIFFRAC.SUITE EVA* software (BRUKER). The peak intensities are related to the size of the coherent scattering domain (CSDS) representing regions of the crystal lattice in which X-ray diffraction is coherent, to the number of crystalline defects, to the presence of the mixed-layering component (e.g. illite/smectite and chlorite/smectite) (Renac and Meunier, 1995) and to the hydration state of these minerals (Ferrage et al., 2007). When the number of coherently stacked sheets is high (i.e broad CSDS), the interference function induces intense and narrow peaks, and then the FWHM is small. Conversely, when the number of sheets is small, the peaks are broader and less intense, the FWHM is wide and the coherent scattering domain is small. In the case of clay minerals in soil, the coherent domain size is generally small except for the primary and phyllosilicates minerals inherited little affected by weathering (Righi et al., 1993; Righi et al., 1995; Lanson, 1997; Chipera and Bish, 2001; Velde and Meunier, 2008; Hubert et al., 2009).

The shape and symmetry of the air dried XRD diffractograms were investigated. The asymmetry of the peak with a broad coherent scattering domain size (CSDS) distribution is due to the presence of several phases with close, but distinct crystallographic characteristics (Lanson and Besson, 1992).

Semi-quantitative estimations of the main clay species were

Please cite this article in press as: El Ouahabi, M., et al., Lacustrine clay mineral assemblages as a proxy for land-use and climate changes over the last 4 kyr: The Amik Lake case study, Southern Turkey, Quaternary International (2016), http://dx.doi.org/10.1016/j.quaint.2016.11.032

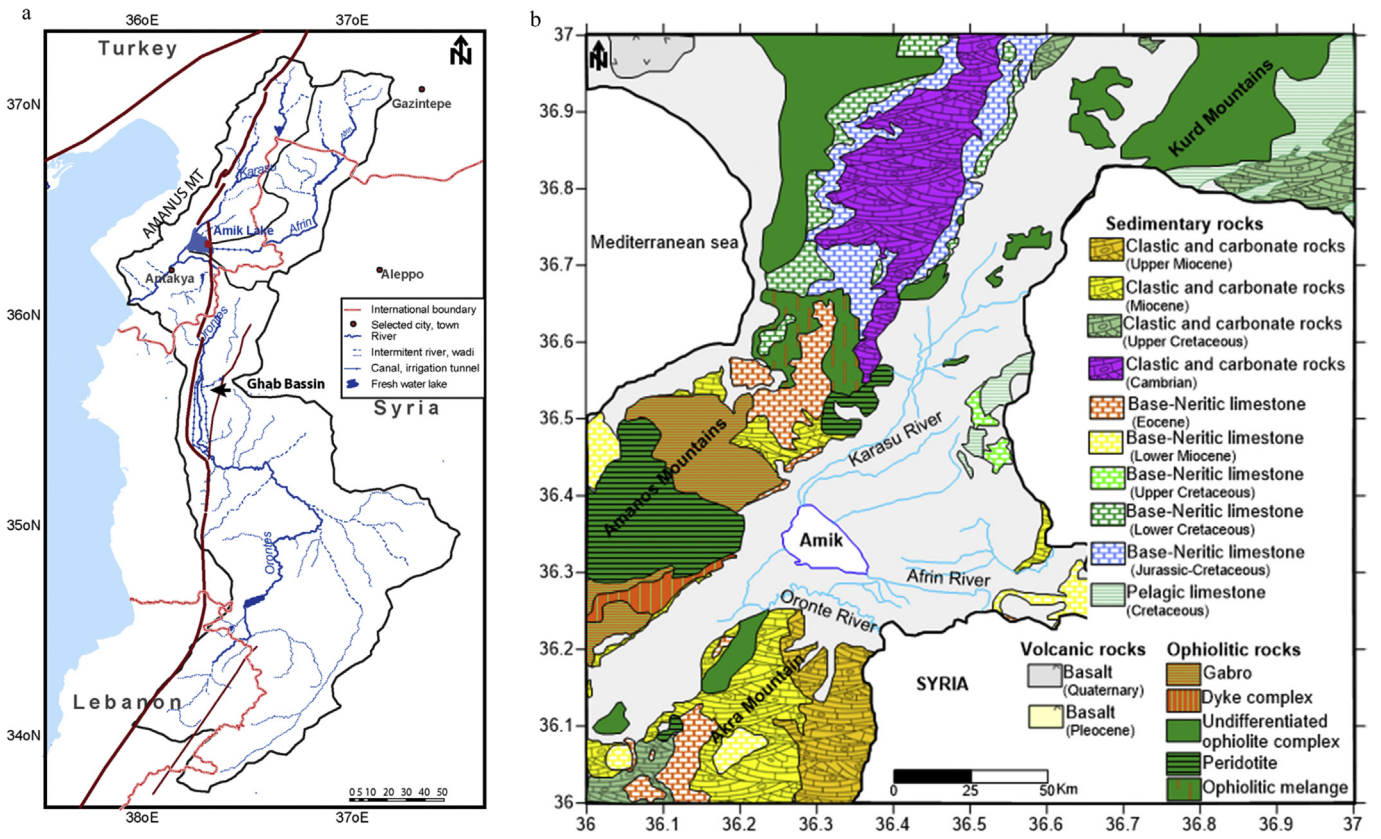

Fig. 1. (a) Geomorphological situation of the Amik plain. (b) Geological context of the Amik Plain.

based on the height of specific reflections on glycolated (EG) runs according to the method of Biscaye (1965), with an estimated uncertainty of ±5%. For calculating relative percentages of the major clay mineral groups present in the given samples, peak intensities were multiplied by the following factors: 0.25 to smectite (17 Å peak), 0.34 to vermiculite (14 Å peak), 1 to illite (10 Å peak) and 0.70 to kaolinite (7 Å peak) and 0.34 to chlorite (14 Å peak) were applied. Kaolinite and chlorite individual percentages were calculated using the 3.54 Å and 3.58 Å peak intensities. Mixed-layer clays amount were estimated using a factor of 0.40 at (~12 Å peak) Biscaye (1965).

The illite chemistry was deciphered by using the ratio of intensities of the 5 Å and 10 Å peaks (Esquevin, 1969). The ratio below 0.5 represents Fe, Mg-rich illites (biotites, micas), which are characteristic for physically eroded and unweathered rocks whereas above 0.5 indicate Al rich illites which are formed by strong hydrolysis (Gingele, 1996). The crystallinity index of illite was measured using the Full Width at Half Height Width (FWHM) of the 10 Å peak in air dried XRD patterns (Kübler and Jaboyedoff, 2000). A high crystallinity index implies a broad coherent scattering domain size (CSDS). The FWHM values of smectite were also calculated.

3.2.2. Radiocarbon dating

The age of the record was constrained using radiocarbon dating. We performed ^{14}C radiocarbon dating (Aeon Radiocarbon Laboratory, USA) on several fractions. Terrestrial vegetal remains provide recent ages linked to the root system developed by agricultural activities in the dried lake after 1940's. The shells are unreliable due to strong and variable reservoir effects (Meadows, 2005). Micro-charcoal remains are the only reliable fraction to date. Four micro-charcoal samples founded in the clayey red levels at 317, 391, 402 and 415 cm depth were dated (Table 1). In addition, some age constraint was provided based on the ^{210}Pb and ^{137}Cs radiometric markers measured every 1 cm from the topsoil to 25 cm. Activities of ^{210}Pb and ^{137}Cs were measured using a low background, high efficiency, well-shaped γ detector (CANBERRA) (Schmidt et al., 2009). Calibration of the γ detector was achieved using certified reference materials (IAEA-RGU-1). Activities are expressed in mBq g−1 and errors are based on 1 SD counting statistics. Excess ^{210}Pb ($^{210}Pbxs$) was calculated by subtracting the activity supported by its parent isotope, ^{226}Ra, from the total ^{210}Pb activity in the sediment (Table 2). The constant sedimentation constant flux model was used to infer an average sedimentation rate (Appleby, 2002).

4. Results

4.1. Lithological description and magnetic susceptibility

Lithology of the core sediments showed small variations with depth (Fig. 3). Silty clay sediments predominated. Sandy particles appeared in some layers or as pockets in the clayey matrix. The colour of the sediment was mostly beige with interposition of reddish and brownish clay levels. Several sedimentary coarser

Table 1
^{14}C Age results obtained from vegetal remains, shells, ostracods and micro-charcoals.

Depth (cm)	Material	^{14}C Age year BP	±	^{14}C Age calBP	±
317	Micro-charcoals	2900	35	3050	62
326	Micro-charcoals	3010	25	3219	43
391	Micro-charcoals	2620	30	2755	10
402	Micro-charcoals	2655	25	2770	11
415	Micro-charcoals	3060	35	3288	47

Please cite this article in press as: El Ouahabi, M., et al., Lacustrine clay mineral assemblages as a proxy for land-use and climate changes over the last 4 kyr: The Amik Lake case study, Southern Turkey, Quaternary International (2016), http://dx.doi.org/10.1016/j.quaint.2016.11.032

Table 2
Bulk activities of ^{210}Pb, ^{137}Cs and ^{228}Th in sediment samples.

Depth (cm)	^{210}Pb (mBq/g)	±σ	^{137}Cs mBq/g	±σ	^{228}Th mBq/g	±σ
2.0	34	2	6.0	0.3	6	0
6.0	19	2	6.0	0.3	7	0
9.0	20	3	6.2	0.5	6	0
11.5	21	4	5.8	0.6	6	1
13.5	15	3	5.6	0.5	6	0
15.5	15	2	5.4	0.4	7	0
17.5	15	4	6.3	0.6	5	1
23.5	12	2	6.0	0.4	7	0
28.5	13	4	4.7	0.7	6	1
33.5	14	3	0.2	0.4	6	1

layers were identified and characterized by coarser grained particles and higher magnetic susceptibility (MS) than the background sedimentation, reworked shells and/or structural disturbances (plastic deformation, sand pillows). Four different sedimentary units (unit 1 to unit 5) were identified based on the lithology, grain-size and MS variation (Fig. 3).

The top unit (unit 5) is 130 cm thick and is mainly sandy clay characterized by an average of MS of 66 ± 16 SI and significant proportion of sand size particles which reach ~80% at 48 cm depth. Below up to 60 cm depth, the profile was characterized by low MS values (63 ± 15 SI, in average) and numerous reworked shells. A slight increase of MS, about 78 ± 15 SI was obtained from 60 to 130 cm depth.

The fourth unit (unit 4) extends from 130 to 196 cm, the sediment is silty clay characterized by a slightly lower values of MS (70 ± 19 SI, in average) showing more variations. Coarse sandy layers followed by silty clay sediment with some sandy intercalations occurred up to 205 cm. Down below and between 205 and 300 cm, sediment is silty characterized by a high MS, not associated with any structural disturbance. Two thin layers showing minor structural disturbances associated with sand were also identified.

The second unit (unit 2) is located between 308 and 450 cm below to the surface, and is characterized by coarser grain-size, a higher MS (132 ± 52, in average), the occurrence of reddish clay levels at the bottom and strong variations in grain size compared to unit 3 (Fig. 3). Several rapid changes in the lithology with various plastic deformations and sand pockets were observed in a clay matrix. Fine red clay layers associated with high MS (231 SI) situated at the base of this unit, between 400 and 450 cm indicating oxic conditions.

The basal unit (unit 1) extends from 450 cm to the bottom of the core, and is characterized by high and variable MS values (96 ± 41 SI, in average), low sand content and the occurrence of reddish clay levels. Sand was mixed evenly with silty clay particles. The core ended with a sandy layer and higher MS values.

4.2. Age-depth model

The age-depth model on the upper part of the core is constrained using ^{210}Pb and ^{137}Cs data (Table 2). Measured ^{210}Pb values in the upper part of sediment core (33.5 cm) range from 34 to 12 mBqg^{-1}. The profile distribution of ^{137}Cs activity shows the maximum at 9 cm depth that represents the period of the maximum 1963 radionuclide fallout. The distribution of excess ^{210}Pb and ^{137}Cs values follows an exponential decrease with depth. Therefore, a constant flux constant supply CS:CR sedimentation model was applied (Appleby, 2002). The ^{210}Pb-derived sedimentation rate (S.R = 0.36 cm/yr) was obtained with ^{228}Th correction. This sedimentation rate implies that the two layers characterized by high MS values between 44 and 66 cm depth, which correspond to two sedimentary events would be induced by the 1872 and 1822 historical earthquakes (Akyuz et al., 2006) (Fig. 2a). The two segments of the Dead Sea Fault, the Karasu and the Hacipasa Faults, have ruptured subsequently in 1822 and 1872 in M ≥ 7 earthquakes (Akyuz et al., 2006). The 1822 earthquake affected most specially the Afrin watershed, and caused landslides (Ambraseys, 1989). Furthermore, the 1872 earthquake triggered liquefactions and ruptured the Hacipasa fault segment (Akyuz et al., 2006) which is a few hundred meters vicinity from our coring site (Ambraseys, 1989).

The age of the lower part of the core is constrained using radiocarbon dating (Table 1). Micro-charcoals at 398 and 408.5 cm provide calibrated ages of 2755 ± 10 and 2770 ± 11yrs BP, implying that the unit 2 was deposited during the Iron Age. The three micro-charcoal samples located above provide older ages by about 400–1000 years, implying large sediment reworking in the watershed. They must be excluded from the age model. At 419.5 cm, micro-charcoal age is 400 years older than the sample located 10 cm above, and is significantly older than the depositional age in the lake.

A composite age model was thus built combining the modern ^{210}Pb sedimentation rate and the two youngest micro-charcoal ages at 398 and 408.5 cm. The modern sedimentation rate was extrapolated to the base of unit 1 at 130 cm depth, where an abrupt decrease in grain-size occurred. Below 130 cm, the sedimentation becomes silty clay, which is coherent with a reduction in sedimentation rate. A constant sedimentation rate constrained by the micro-charcoals from 130 cm to the base of the core is considered. Given that our age model is constrained at the top and at the bottom, its greatest uncertainties are associated with the Islamic period in the middle of the section.

The age model may appear imprecise, but it is compatible with the sedimentary history established in previous studies in the east part of the Amik basin near the coring site. First, the nearby large Bronze Age site of Karatepe tell (AS 86) was made of lacustrine grey silty clay, which could be the clayey unit 1 (Fig. 3). Second, at the end of the Roman period, the lake level increased above the sandy ridge limiting the former lake, as a result the cultivated lands to the east of the coring site where inundated with grey silt lacustrine marl overlying formerly cultivated soils (Yener et al., 2000). The lake level increase is recorded in the unit 3 attested by the fine-grain sedimentation, which corresponds to the Late Roman Period in our age model. Third, during the Ottoman/Islamic Period, another environmental change occurred: silty clay derived from the Afrin River overlies the lacustrine clay deposited since the end of the Late Roman Period (Yener et al., 2000). This change occurred after the travel of Abu-al Fida at the end of the 13th century in the region (Eger, 2011; Casana, 2014). This transition is also recorded at our site between the silty clay unit 4 and the silty sand unit 5. According to our age model, it would have occurred around 1650 AD, an age compatible with historical data.

4.3. Identification and characterization of the clay minerals

Smectite (0–60%), illite (5–50%), kaolinite (5–30%), chlorite (0–45%) and vermiculite (0–65%) were the main clay minerals present in the Amik Lake sediments. Mixed layers clay minerals were also present. There were mainly chlorite/smectite interstratified (0–25%) accompanied by the appearance of illite/smectite interstratified clay minerals (0–30%) in the upper part of the core.

The XRD patterns of air dried clay samples had strong first-order reflections with various basal spacing and peak intensities that are described in the following. We also evaluate the crystallinity of the phyllosilicates based on the peak shapes, broad or narrow, and the peak asymmetry in the d(001) basal diffraction and the size of the

Please cite this article in press as: El Ouahabi, M., et al., Lacustrine clay mineral assemblages as a proxy for land-use and climate changes over the last 4 kyr: The Amik Lake case study, Southern Turkey, Quaternary International (2016), http://dx.doi.org/10.1016/j.quaint.2016.11.032

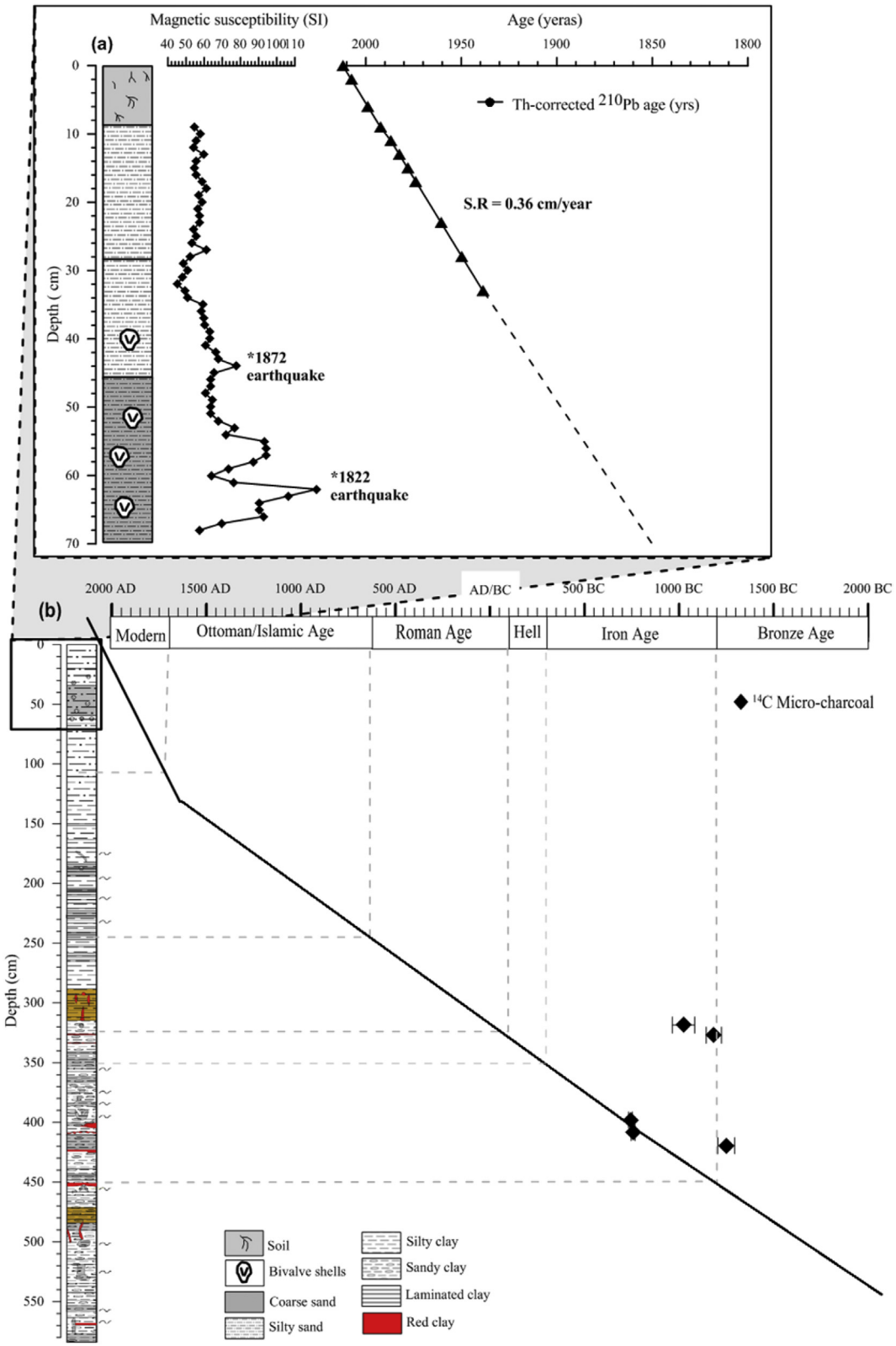

Fig. 2. (a) Sedimentation rate and age–depth model from radionuclides (^{210}Pb), a constant sedimentation rate was calculated and corrected by ^{228}Th activity. The highest magnetic susceptibility peak values are used as earthquake tie-point to extrapolate the sedimentation rate. (b) Age-depth diagram for Amik Lake based on calibrated ^{14}C age results obtained from micro-charcoal remains, ^{210}Pb activity and historical earthquakes tie-point (data from Akyuz et al. (2006).

coherent scattering domain size (CSDS) distribution.

Most of clays showed a broad basal reflection d(001), ranging from 13 to 16 Å, characteristic of smectite. Smectite had, generally, broadened reflection, asymmetrical or near asymmetrical (Fig. 4). The distinction of smectite from vermiculite and chlorite was based on the expansion of the d(001) reflection to 14-18 Å upon ethylene

Please cite this article in press as: El Ouahabi, M., et al., Lacustrine clay mineral assemblages as a proxy for land-use and climate changes over the last 4 kyr: The Amik Lake case study, Southern Turkey, Quaternary International (2016), http://dx.doi.org/10.1016/j.quaint.2016.11.032

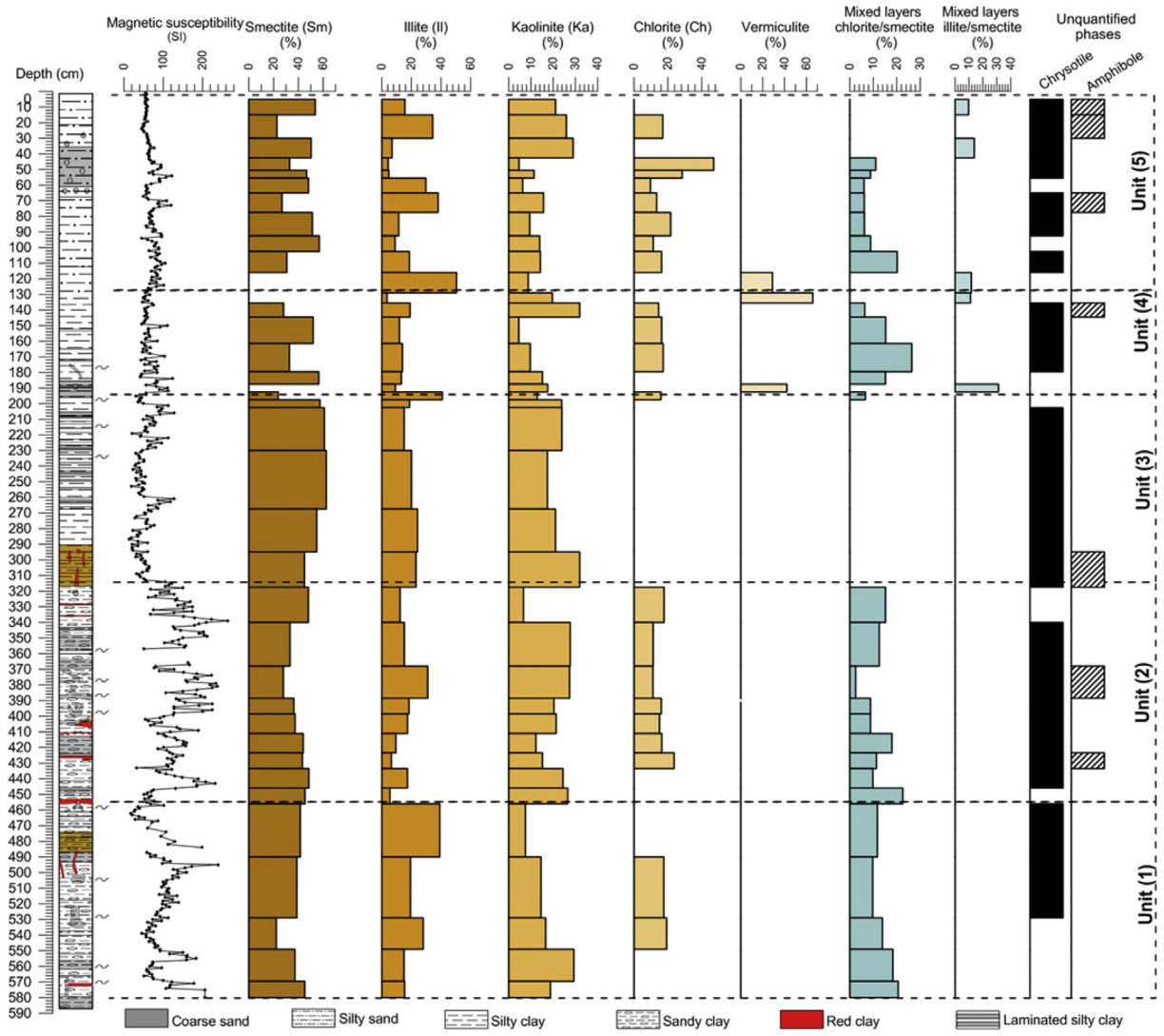

Fig. 3. The main clay mineralogical composition and magnetic susceptibility of the Amik Lake sediments in terms of depth variation.

glycol saturation run, and on the collapse to 10 Å after heating at 500 °C for 4 h. The observed asymmetry of the d(001) peaks of smectite towards low angles is due to the contribution of a low CSDS particle population to the diffracted intensity (Fig. 4) (see Fig. 5).

Kaolinite was detected in all clay samples and showed in air dried and glycolated spectra characteristic peak around 7.05 Å d(001) and 3.52 Å d(002) reflections occurring at 12.4 and 24.9 2Theta, respectively. The d(001) and d(002) peaks did not change on ethylene glycol saturation (EG) meaning that no swelling occurs. After heating at 500 °C, the peak disappeared pointing out the kaolinite transformation into metakaolinite (dehydroxylation) and the absence of well crystallized chlorite. Two peaks were observed at ~ 7 Å (Fig. 4). The peak at ~7.30 Å may be related to chrysotile, whereas the peak at ~7.05 Å is typical of the authigenic kaolinite. No significant peak asymmetry change was observed for the 7.05 Å peak of kaolinite and the coherent domain size was generally broad; kaolinite was thus a primary less weathered mineral.

Illite was present in most of the samples and was distinguished by the d(001) reflection at around 10 Å. The peak remained unaffected by the ethylene glycol treatment and the heating at 500 °C. The sharp and the broad d(001) and d(002) peaks at ~ 10 Å and ~ 5 Å, respectively, do not shifted after glycol solvation (Fig. 4). The peak asymmetry was observed and is related to the presence of phases with close, but distinct crystallographic characteristics like illite and detrital mica (Lanson and Besson, 1992).

Chlorite and vermiculite were also detected and were characterized by a broad d(001) basal reflection at ~ 14 Å under the air dried, ethylene glycol saturation and heated treatment. It is rather difficult to distinguish the chlorite reflection due to the co-existence of the broad d(001) reflections of smectite and chlorite in the same sample. Chlorite can still be clearly identifiable because (1) it is relatively thermally stable and thus resistant to heating at 500 °C, (2) it shows a peak at ~ 14 Å after ethylene glycol saturation characteristic of chlorite minerals (Fig. 4). The weak peak of chlorite around ~14 Å is asymmetric, reflecting poor crystalline species and the contribution of chlorite with a small coherent domain size (CSDS). This indicated that the deposited chlorites were transformed by weathering after their formation. Vermiculite could be identified readily based on the collapse of the peak at ~14 Å to 10 Å after heating at 500 °C. The peak of vermiculite was symmetric at ~14 Å under air dried and ethylene glycol saturation but was large at the base due to its hydration. The symmetry of the vermiculite peak and its large coherent domain size (CSDS) indicates their primary origin (Fig. 4a).

Please cite this article in press as: El Ouahabi, M., et al., Lacustrine clay mineral assemblages as a proxy for land-use and climate changes over the last 4 kyr: The Amik Lake case study, Southern Turkey, Quaternary International (2016), http://dx.doi.org/10.1016/j.quaint.2016.11.032

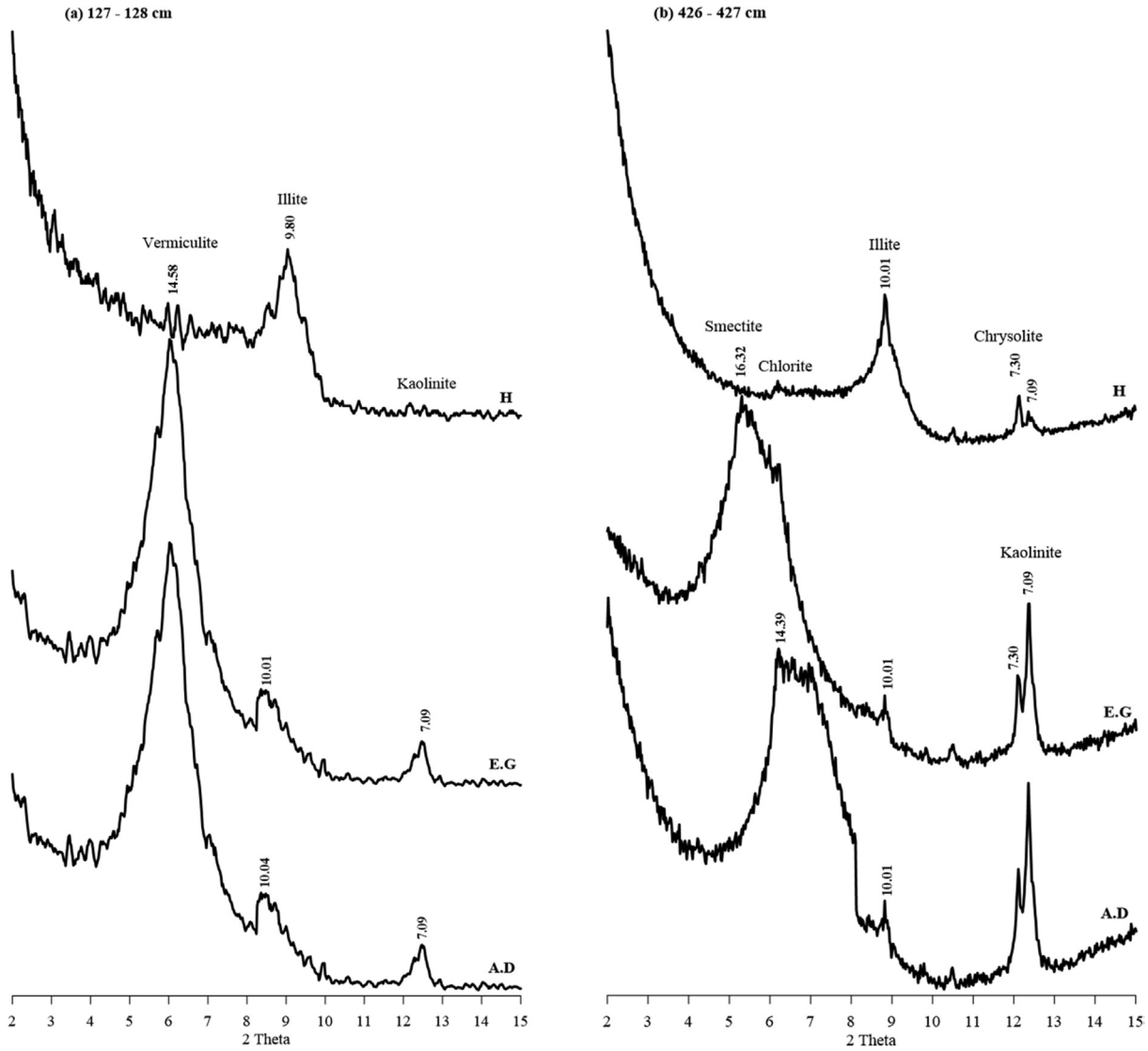

Fig. 4. X-ray diffraction (XRD) patterns of the clay fraction (<2 μm) of the depths of 426–427 cm. A.D: oriented preparations in the air-dried; EG: ethylene-glycol solvated state; H: Heated at 500 °C for 4 h.

Regarding to the characterization of the mixed layer clay minerals, the air-dried patterns towards low angles produced a broad and asymmetric reflection between ~10 and ~14 Å due to the presence of several phases with distinct crystallographic characteristics (Lanson and Besson, 1992). This behaviour, according to the methods proposed by Moore and Reynolds (1997) and Thorez (1976) enabled the distinction of three mixed-layered structures often associated with discrete mineral phases: illite/smectite, chlorite/smectite and illite/chlorite. Illite/smectite interstratified clays. These mixed layer clays are characterized by an expanding to higher spacing under ethylene glycol saturation, and a collapse to 10 Å under heating at 500 °C. In addition, and according to (Inoue et al., 1989), the high saddle/peak ratio close to 17 Å and the appearance of an 8.6 Å peak at 10.3 2Theta on the EG pattern reveals that the clay sample was composed of randomly interstratified illite/smectite mixed layers (Reynolds, 1988). The presence of a super structure reflection at ~29 Å which shifted to ~31 Å after the ethylene glycol run indicated ordered chlorite/smectite mixed layer (Reynolds, 1988). Mixed-layer species were thus mainly chlorite/smectite and illite/smectite phases and are attributed to a soil source (Righi et al., 1995). Traces of chrysotile and amphibole were also founded. These relict fractions would come from the ophiolite body located just to the west of the Amik Plain.

4.4. Evolution of the clay minerals

The clay phases (<2 μm fraction) significantly differed throughout the core sediments. In addition, the crystallinity of illite as well as the shape of the air dried and glycolated XRD diffractograms of the overall phyllosilicates were quite different, mainly related to different mode of stacking of the phyllosilicates sheets. In general, in the Amik lake sediments only kaolinite has a high CSDS (FWHM < 0.3° ± 0.2°). Six units could be distinguished regarding to the evolution of clay mineral species with depth:

In unit (1), the main abundant clays were composed, in average, of smectite (37 ± 9%), illite (23 ± 10%), and kaolinite (17 ± 8%), with the presence of the chlorite/smectite interstratified clays (15 ± 5%). About 20% of chlorite was present in 319–339 cm depth interval (Fig. 3). The FWHM values of smectite (~1.3 ± 0.2°) were high compare to the other units, indicating that the smectite particles were thicker. The unit was characterized by an upward increase of

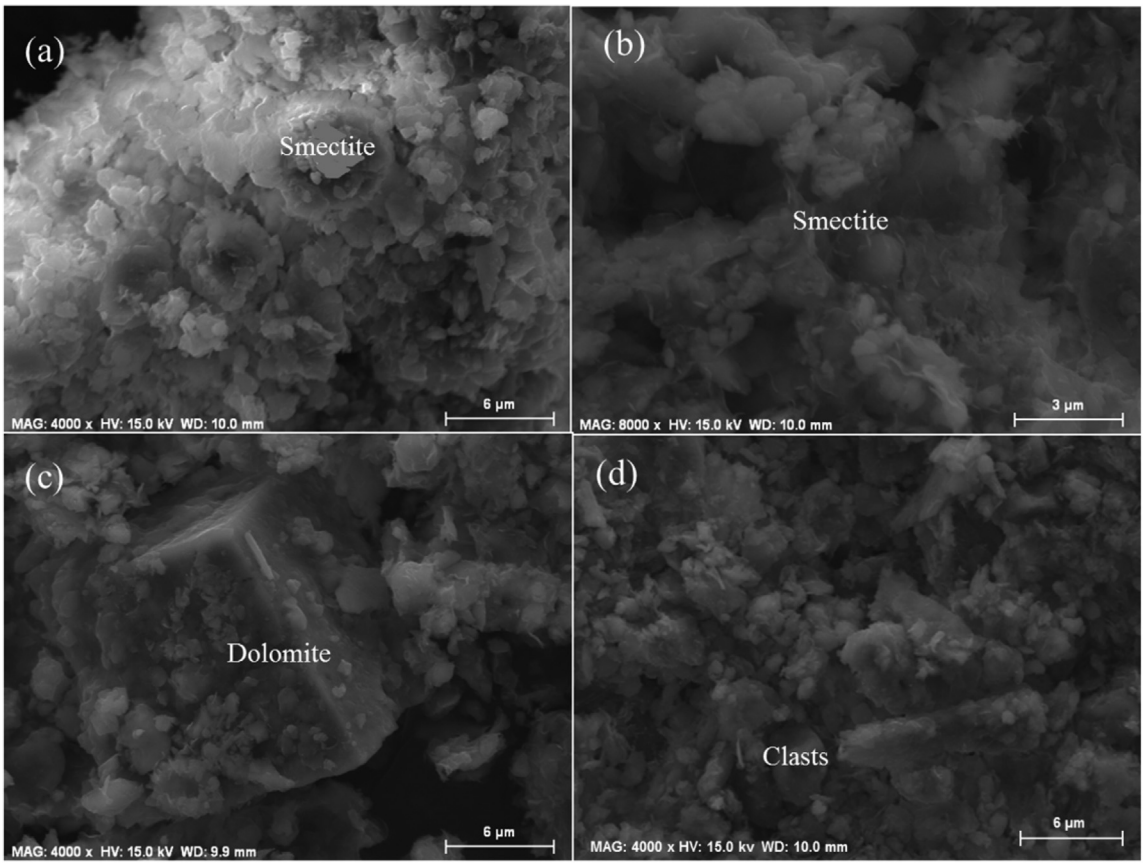

Fig. 5. Scanning electron micrograph of bulk sediments indicating: (a) and (b) detrital clays are dominated by smectite at 89 cm depth; (c) detrital clays cover an crystal of dolomite at 129 cm depth; (d) detrital clays and others clasts at 129 cm depth.

illite in parallel with a decrease of kaolinite and chlorite/smectite mixed layer clays The FWHM values of illite were low and vary, having an average value of 0.5 ± 0.2°, and decreased at the top to this unit. The illite chemistry showed an anomalous interval around the depth of 520 cm with a high value of 1.8, indicating a strong chemical weathering (Al-rich illite); at other depths it had low values around 0.4 indicating a weak hydrolyse and a significant contribution of Mg-rich illite.

In the unit (2), the clay fraction comprised smectite (41 ± 7%), kaolinite (20 ± 8%), illite (14 ± 8%), chlorite (12 ± 8%) and chlorite/smectite mixed layers (13 ± 6%). An increase of illite was recorded in the middle of the unit; this rise was associated with a slight decrease in the smectite amount. The FWHM values of illite were low about 0.4 ± 0.2° and gradually diminished upward indicating an increasing crystallinity of illite; illite chemistry showed basal high values reaching 1.7 around 440 cm and then a sharp fall to values around 0.4 indicating an increase in Mg-rich illite.

Smectite was the main clay in the unit (3), with an average of about 51 ± 15%. Kaolinite (22 ± 7%) and illite (24 ± 9%) were the other clay fraction present at this unit; chlorite and mixed layers were absent. The FWHM values of illite showed little variability around 0.4° ± 0.1°. A slight decrease of the crystallinity of illite was recorded at the top of this unit, associated with a small rise in illite chemistry indicating an Al-rich illite formed by chemical weathering. The boundary between the units (3) and (4) was anomalous with the reappearance of chlorite and mixed layer, and the punctual transformation of smectite into vermiculite.

In unit (4) various changes in clay mineral assemblages occurred as well as another anomalous interval. Smectite is the main clay mineral (24 ± 25%, in average). Illite content was also highly variable with average values of 17 ± 15%. Its FWHM values were low (0.3 ± 0.2°) and fluctuating. The illite chemistry was variable, but generally low (<0.5) indicating that Fe and Mg-rich illite was formed. The other main clay mineral was kaolinite (15 ± 9%, in average), chlorite (7 ± 9%, in average), chlorite/smectite mixed layers (9 ± 10%, in average). The anomalous interval between 140 and 105 cm depth showed the punctual appearance of vermiculite and mixed layers illite/smectite (8 ± 12%), the disappearance of smectite and the presence of Fe and Mg-rich illite with an intermediate crystallinity. This anomalous interval was similar to the one at ~190 cm.

The unit (5) involved variations in the clay minerals composition. Smectite (42 ± 17%), illite (17 ± 13%), kaolinite (11 ± 4%), chlorite (21 ± 13%) and clay mixed layers (10 ± 15%) were the main clay components. An increase in kaolinite content from 40 cm to the surface is observed. However, a sudden fall in kaolinite and illite occurred between 40 and 6 cm depth. The crystallinity of illite was high at the base; its chemistry indicated Mg–Fe rich illite. The unit showed an anomalous interval around 60 cm with the occurrence of Al-rich illite. The crystallinity of illite (FWHM = 0.5 ± 0.1°) was higher from 50 cm to the surface. It chemistry was relatively high at the base indicating Al-rich illite and low at the top suggesting the occurrence of Mg–Fe rich illite.

5. Discussion

5.1. Provenance of the Amik clay sediments

Clayey deposits can be formed by a wide various sources and dynamics, such as erosion-deposition of weathered rocks or soil e.g.

Please cite this article in press as: El Ouahabi, M., et al., Lacustrine clay mineral assemblages as a proxy for land-use and climate changes over the last 4 kyr: The Amik Lake case study, Southern Turkey, Quaternary International (2016), http://dx.doi.org/10.1016/j.quaint.2016.11.032

(Moss and Walker, 1978; Dotterweich, 2008; Tsatskin and Zaidner, 2014), inheritance of soluble minerals after limestone dissolution as well as by neoformation. In this study, the observed clay crystallinity as well as their XRD diffractogram shape imply that clays are mostly detrital that originated dominantly from the erosion of the surrounding soils and geological rock formations, reflecting the geology and soil cover in the lake catchment (Fig. 5). Multiple sourced inputs thus exist (Fig. 3). The proximal sources are the Amik Plain and its immediate surrounding composed of a large diversity of geological outcrops forming mountain ranges and plateaus (Fig. 1a). Clay sources extend potentially on a much larger area as the Amik Lake. The Amik Basin is watered by three large rivers having large watersheds. To the south of the Amik Plain, the Orontes is the largest river with a catchment size of 24 660 km^2 composed mostly of limestones, marls, amphibolites and schistes (Lehner et al., 2008). To the north, the Karasu drains a catchment of 450 km^2 composed of rocks with similar geology to the Amanus Basin as well as recent volcanic rocks (basalts); to the east, the Afrin River drains mostly calcareous and ophiolitic rocks (Fig. 1b). According to the present soil map, the Amik Plain and its three rivers catchment, show poorly developed soil (entosols and some inceptisols in the Afrin catchment) except in the lowland along the Orontes; this is consistent with the semi-arid environment of the most of the Amik catchment (Kilic et al., 2006). The geomorphological study of (Casana, 2008) showed that several episodes of soil development and erosion occurred in the last 3000 years just to the south of the Amik Plain.

The detrital clays in the Amik Lake would express the weathering conditions at the source. The clay types found shows that chemical weathering products (smectite and kaolinite) dominate over the physical weathering products (illite and chlorite) in the Amik Basin (Chamley, 1989). Chemical weathering is indeed foreseen given the climate regime of the Amik Plain, which is a typical Mediterranean climate, with a large annual precipitation (~1000 mm/yr), an 18 °C annual average temperature, and 69% relative humidity (Gün and Erdem, 2003). In the following, the clay major sources are identified and discussed based on the clay minerals abundance and their characteristics.

Illite is generally considered primary minerals derived from the degradation of metamorphic and igneous formations as well as from the erosion of sedimentary rocks (Chamley, 1989). The relatively high crystallinity index of illite in some samples (FMWH between 0.2° and 0.4°) shows that a significant proportion of the illite is probably derived from the weathering of the metamorphic rocks (biotite and feldspars) in the catchment (Righi et al., 1995; Lanson, 1997; Chipera and Bish, 2001; Hubert et al., 2009). However, in the Amik catchment, the broad base peaks of illite show that illite is mostly detrital with a FMWH greater than 0.4 (Pandarinath, 2009; El Albani et al., 2011). The small coherent domain size confirms that part of illite results from a transformation within a soil formation context and reflects weathering (Lanson and Besson, 1992). The recurrent occurrence of Mg and Fe-bearing illite is traditionally interpreted as a proxy for physical weathering, but in the present Mediterranean climatic context this interpretation is questionable. The documented Mg and Fe-bearing illite would still indicate a weak hydrolyse but suggest the input of detrital iron-rich illite that is present particularly in the Late Cretaceous marine chalks from the Arabian plateau in the Afrin catchment.

Chlorite is generally derived from in igneous rocks as an alteration product of mafic minerals such as pyroxene, amphibole and biotite, as well as from the erosion of sedimentary rocks (Chamley, 1989). In our context, chlorite would be produced by alteration of mafic rocks having high iron and magnesium content (e.g. ophiolite) (Biscaye, 1965; Singer, 1984; Buurman et al., 1988; Chamley, 1989). The broad shape of the peaks of chlorites and their weak crystallinity confirm their detrital origin. The Kurd, Amanus and Akra Mountains are thus the potential sources of chlorite. The absence of chlorite mostly during the deposition of unit (3) and unit (5) indicates probably a cut-off of those sources that would be discussed in the next section.

Smectite is generally considered to be a secondary mineral that is the product of pedogenetic weathering. Smectite is derived mostly through chemical weathering of volcanic rocks in temperate and sub-arid zones (Chamley, 1989; Weaver, 1989; Fagel et al., 2003). In the Amik Plain, smectite is detrital and can have a wide range of sources brought by the three major rivers flowing into the plain. It could be derived from a) ophiolite complex (amphibole and pyroxene), b) alteration of volcanic rocks along the Karasu valley, c) sedimentary deposits present in the three river catchments. During the deposition of unit 3, the percentage of smectite was particularly high suggesting a strong input from these sources excluding the ophiolite body, which would also produce chlorite.

Kaolinite is also considered to be a secondary mineral that is the product of pedogenetic weathering, derived through chemical weathering of parent aluminosilicate under warm and humid conditions (Weaver, 1989; Fagel et al., 2003). Two kaolinite populations were founded in the Amik Lake sediments: a detrital and neoformed. This interpretation is based on the shape of the d(001) peak of kaolinite which is narrow at the top and more large at the base in the XRD spectra. The detrital fraction of kaolinite is undoubtedly a reworked fraction coming from Cretaceous and Cenozoic sedimentary rocks that contain a significant proportion of kaolinite (Fig. 1a) and from the weathering of igneous rocks rich in feldspars and other aluminous minerals and poor in ferromagnesian minerals in vicinity of the ophiolite complex situated in the Amanus, Kurd and Akra Mountains. The neoformed kaolinite fraction is post-depositional formed during weathering.

Chrysotile is detrital derived from the serpentinisation process from the ophiolite rocks, especially from olivine by alteration (Prichard, 1979). The traces of amphibole relict are derived from the ultramafic rocks and the ophiolitic belts located in the watershed.

Finally, the occurrence of mixed-layer clays in the Amik Lake sediments indicates that the developed soils in the Amik watershed were eroded. Such erosion would be triggered, for example by agriculture, wood exploitation and mining. The presence of mixed layer clays through most of the core show that an intensive erosion of fertile soils has occurred from the catchment to the Amik Lake for a long time as confirmed by other studies (Wilkinson, 1999; Casana, 2008). The mixed layers, which are a product of soil erosion, are absent during the Roman period; the later suggest that the clay source of the Amik Lake was changed during that period. Chlorite source has been disrupted as well during the same period. The unchanged weathering proxies (illite chemistry, Sm/Il ratio) during the unit 3 compared to the previously deposited unit 2 further suggests a change in the source area.

5.2. Evolution of the environmental conditions during the last 4 kyr

The major clay minerals, smectite, illite, kaolinite and chlorite showed significant changes in the studied core. Their relative abundance may be taken as a proxy for chemical weathering rate in the watershed: a high percentage of smectite and kaolinite would reflect warm and wet climate conditions. Furthermore, crystallinity and chemistry of illite could provide complementary information regarding the weathering conditions, which are sensitive to the climate change (Chamley, 1989; De Visser and Chamley, 1990; Pandarinath, 2009). Low illite crystallinity is generally associated with greater chemical weathering (Pandarinath, 2009), induced by high temperature and significant rainfall. On the opposite, the

Please cite this article in press as: El Ouahabi, M., et al., Lacustrine clay mineral assemblages as a proxy for land-use and climate changes over the last 4 kyr: The Amik Lake case study, Southern Turkey, Quaternary International (2016), http://dx.doi.org/10.1016/j.quaint.2016.11.032

crystallinity of illite increases during colder and drier conditions (Fagel et al., 2003). Smectite/kaolinite (Sm/Il) and kaolinite/illite (Ka/Il) ratios can be used as proxy to discuss the climatic conditions indicating chemical weathering. Sm/Il and Ka/Il ratio evolved in the same way in the Amik Lake sediments, here we use only Sm/Il ratio as proxy. In addition, Sm/(Il + Ch), Ka/(Il + Ch) are used as weathering proxies.

Based on the obtained age model, we considered that the sediment deposited through the unit 1 corresponds to the Late Bronze Age (2000–1200 BCE); the unit 2 corresponds to the sediments deposited throughout the Iron Age (1200–300 BCE) and Hellenistic period (300 BCE – 100 BCE), the unit 3 was deposited during the Roman and early Islamic periods (100 BCE – 650 AD); the unit 4 comprises the sediment from the Islamic and Ottoman periods (650 AD – 1650 AD); the unit 1 represents the Modern period.

The temporal variations in clay mineralogy are discussed throughout these archaeological periods and the wealth of existing data regarding the human occupation in the Amik Plain and climatic change during the last 4000 years. We particularly looked at some possible cause-and-effect relationship between land-use, climate and soil erosion products supplied in the Amik Lake sediments during the different periods since the Late Bronze Age.

5.3. Bronze and iron ages

The high magnetic susceptibility during this period highlights the occurrence of strong erosion. The relatively high amount of chlorite/smectite mixed layers suggests sustained soil erosion with a detrital source composed of developed soil levels (Righi et al., 1995). The Amik plain was heavily settled with hundred or more settlements occupied at some point during second millennium BC (Casana, 2009), as well as the Orontes and Afrin catchments. Soil erosion during that period would be linked to deforestation in the Amik catchment that is attested by the pollen record in the Ghab Basin flowed by the Orontes to the south of the Amik Plain (Meadows, 2005). Marriner et al. (2012) documented during that period a large increase in sedimentation rates on the nearby Syrian coast induced by soil erosion in local catchments. In the Amik Plain, the sedimentary record of Wilkinson et al. (2001) shows a high chromium content during the Bronze and Iron Ages that was related to soil erosion in the Amanus Mountains in relation with deforestation and the exploitation of ores. The occurrence of thin red clay layers in the core during this period, which clay characteristics are not different from the other layers, could be related to the erosion of red soil founded in the Mediterranean area, and particularly in the Afrin catchment that likely developed during the Tertiary and Quaternary hot and humid periods (Atalay, 1997). The low amount of illite and the absence of chlorite during the Bronze Age and at the transition between Bronze/Iron suggest a decrease in erosion and a change in land-use.

Regarding climate, Drake (2012) shows that in the eastern Mediterranean a warm climate was prevailing during the Bronze Age, and a cool and more arid climate during the Iron Age which lasted until the Roman warm Period. Climatic proxy in coastal Syria suggests that drier climatic conditions occurred in the Mediterranean belt of Syria from the late 13th/early 12th centuries BC to the 9th century BC (Kaniewski et al., 2010). During the beginning of the Late Bronze Age (bottom of the sediment core), the high amount of kaolinite and small rise of Sm/Il ratio associated with relatively high illite crystallinity suggest more chemical weathering. This indicates that climate was warm during that period.

The Bronze-Iron transition is marked by large variations in the clay minerals content and illite crystallinity. The very low kaolinite content, the narrow FWHM and the low illite chemistry (iron bearing illite) suggest dry climate conditions. The end of the Bronze Age and the beginning of the Iron Age have been described as a Dark Age related on one hand to the collapse of the Hittite Empire and on the other hand to climatic changes (Weiss, 1982; Drake, 2012). Settlement studies around the Amik Plain suggest no major disruption: the Bronze-Iron Ages were characterized by an occupation of the low lands, with deforestation in the mountains, particularly the Amanus Mountains (Casana, 2008). There was a possible decreasing settlement density at the end of the Bronze Age, but no identified societal changes (Casana, 2007, 2012). The paleoethno-botanical work of Capper (2012) indicates a lack of agricultural variation in the area. Agriculture was mainly developed in the lowland areas, and was sustainable in the fertile Amik Plain during drought periods (Casana, 2012).

During the early Iron Age, the kaolinite content, Sm/Il ratio, Sm/(Il + Ch) and Ka/(Il + Ch), increased significantly and suggest a more intense chemical weathering associated with more leaching in the watershed. Furthermore, at this time, illite had a low crystallinity (high FWHM) indicating an enhanced chemical weathering of the stack of phyllosilicates sheets due to warm and humid conditions. During the later Iron Age period, drier conditions occurred, attested by a significant decrease in illite chemistry, Sm/(Il + Ch) and Ka/(Il + Ch). The strong decrease in the FWHM related to an increase in illite crystallinity and illite chemistry (Fe–Mg-rich illite) all point to less favourable climatic conditions, ie. cold and dry. Finally, there are more rapid changes in the clay types, abundances, Sm/Il ratio and illite crystallinity during the Iron Age than during the Bronze Age, suggesting that a significant climatic variability but unchanged source areas.

5.4. Roman age

The Roman period is drastically different from the preceding Iron/Bronze Ages regarding clay minerals composition as well as magnetic susceptibility data. The absence of interstratified clays and chlorite suggests a change of source or soil erosion pattern during that period, characterized by the lack of input of developed soil levels already formed that are usually related to intense erosion. The low magnetic susceptibility values during this period confirm a weak terrigenous input to the lake. These facts seem at odds with the human occupation at that time. The Roman period coincides, in fact, with the strongest anthropogenic pressure that had occurred through the whole history of the Amik watershed (Casana, 2007; Yener et al., 2000; Wilkinson and Rayne, 2010). The development of the city of Antioch with a large population had led to the development of a more intensive agriculture/arboriculture covering the lowland and the highlands as well as the development of a complex network of irrigation (Izdebski et al., 2016). In particular, settlements expanded on the shoulders of the Orontes valley and pasture in the upland areas were converted to arboriculture (Casana, 2007; Izdebski et al., 2016). The apparent contradiction between restricted soil erosion and an intense land-use was already point out by Casana (2008), which suggested that Roman and late Roman land-use created the necessary preconditions for soil erosion to occur, but that erosion actually took place about 400 years after settlement in the Amik highlands under a different climate regime. The specificity of the Roman period around the Amik Lake is also attested by the occurrence of a mature soil at the foot of the Amanus Mountains that developed during that time (Yener and Batiuk, 2010). The paleosoil overlained gravels deposited during the Bronze/Iron period and is covered by even coarser gravels deposited again during the Early Islamic period. This buried Roman land surface has a significant extent and attests of a unique long period of non-erosive conditions (Eger, 2011). In fact, in erodible Mediterranean landscapes, unprotected soils under

Please cite this article in press as: El Ouahabi, M., et al., Lacustrine clay mineral assemblages as a proxy for land-use and climate changes over the last 4 kyr: The Amik Lake case study, Southern Turkey, Quaternary International (2016), http://dx.doi.org/10.1016/j.quaint.2016.11.032

pastures show the highest degree of erosion among the various types of land use (Marathianou et al., 2000). The development of arboriculture in highlands associated with terracing on steep slope would not enhance, but reduce erosion. Marathianou et al. (2000) noted on the Levsos Island in the Aegean Sea that soils under pastures are thin and more erodible than soil occupied by olive trees with terracing and that the developing of a livestock farming can protected land from soil erosion. Similarly the study of Özşahin and Uygur (2014) in the mountainous range south of the Amik Plain shows that wheat growth as a crop can reduce erosion.

We could identified three possible concurrent factors that may be responsible for observed change in clay minerals during the Roman period: (1) landscape stability linked to low climatic variability (storminess); (2) intense human terracing on the upslopes and highlands that prevent soil erosion despite an intensive land-use; (3) channelization of the rivers draining the Amik plain resulting in a shift in the sediment sources in the Lake. The Afrin River which enters the Amik plain at it southern eastern corner was fully channelized, triggering the development of settlements to the east and north-east of the Amik Lake (Wilkinson and Rayne, 2010). At least three channel networks were built in different phases, the earliest ones at the beginning of the Roman period (Yener and Yener, 2005; Gerritsen et al., 2008; Wilkinson and Rayne, 2010; Eger, 2011). Some of these channels were used until the early Islamic period (Yener and Yener, 2005; Gerritsen et al., 2008; Wilkinson and Rayne, 2010; Eger, 2011).

5.5. Islamic age

The end of the Roman period and the beginning of the Islamic one (Roman/Islamic transition) were marked by a strong decrease in the settlement density in the Amik Plain (Yener et al., 2000) as well as in the highlands of the Afrin and Orontes watersheds (see Dead cities in Casana (2014)). The population decline is probably linked to the much diminished economic and political role of the Antioch city (Liebeschuetz, 1972) at that time and to an epidemic of plague and repeated destructive earthquakes rupturing the Dead Sea Fault that devastated the region (Marco, 2008; Altunel et al., 2009). These combined factors would have a high toll on the population and settlements, and thus on the land-use during that time. The intensive agriculture and arboriculture sharply declined and pastoralism developed (Kaptijn et al., 2013).

During the Roman/Islamic transitional period (Roman/Islamic), smectite was transformed into illite/smectite interstratified and chlorite into vermiculite. Colder conditions would have taken place during this critical period. Haldon et al. (2014) indicates that the climate became much colder during the first half of the sixth century in the eastern Mediterranean Area.

The Islamic Age is globally characterized by the renew appearance of mixed layer clays indicating a renew erosion of mature soil in the catchment similar to the one during the Iron-Bronze Ages. The low magnetic susceptibility values during that time still suggested moderate soil erosion compared to the Iron/Bronze Period. This erosive period is responsible for the burial of the Late Roman settlements, and of the Roman Antioch City, which rests below 6 m of alluvial sediments of the Orontes (Casana, 2007). The renew erosion would be related to the increase of pastures and the decrease in the management of terraced terrains in the highlands (Marathianou et al., 2000). Terraces are agricultural structures built to protect the soil from erosion and to increase the terrain productivity, but they need a sustained maintenance, which may not be feasible given the decrease in sedentary population during the Islamic Period. Their abandonment would result in enhanced soil erosion by run-off water as observed in the present record.

The complete change in clay mineralogy from Roman to Islamic time could be related to other concurrent local and/or global factors. Three additional local factors could be identified. The first one would be the siltization of channels feeding the coring site, and possibly of other channels on the Afrin or Orontes Rivers. In the Amik Plain, a marshy landscape prevailed starting in the early Islamic time and expanded in the later periods (Yener et al., 2000). The second one would be the renewed exploitation of forests in the mountains as a source of wood. During Middle Age, Amanus was heavily exploited for its wood and Antioch was a large wood market for Central Syria and Mesopotamia (Lombard, 1959). The third possible factor would be the occurrence of repeated strong earthquakes that impacted the landscape and the river network. Cluster of three to four large $M > 6.5$ earthquakes during the 6th century stroke Antakya and its surrounding, the largest one occurred on May 29 526 or 525 and would have killed about 250 000 people (Guidoboni et al., 1994; Ambraseys and White, 1997; Akyuz et al., 2006). In addition, strong earthquakes have the potential to divert the river drainage, which would affect the clay type input into the Amik Lake; the later occurred during the historical 1822 and 1872 earthquakes (Ambraseys, 1989). Finally large magnitude earthquakes shatter the landscape, preferentially affecting the mountain regions, like the Amanus. There, earthquake strong ground motion would trigger extensive slope failures and enhance the erodibility of rock and soil (Harp and Jibson, 1996). The strong shaking of the landscape would thus increase the sediment flux into the Amik Basin, a phenomena that have been documented after recent earthquakes (Hovius et al., 2011). The concomitant seismically induced erosion, deforestation and the permanent failure of infrastructures capable to keeping the sediments on the highlands and slopes must have play a role in the renewed input of soils in the Amik Lake. Global factors, i.e climate, could also play a role regarding the observed change in clay mineralogy. Cooler conditions would have occurred during the Roman/Islamic transition, as indicated by the transformation of chlorite into vermiculite, a fall in Sm/Il ratio and Sm/(Il + Ch). Similarly, McCormick et al. (2012) have evidenced that increased in the Western Roman Empire (around 400 AD) indicating colder and wetter conditions.

During the Islamic time, some changes in clay mineralogy may also be indicative to climate change. During the early Islamic period an increase in the Sm/Il ratio and Sm/(Il + Ch) is recorded, indicating more chemical weathering due to warm climate. Moreover, a slight decrease in the crystallinity of illite also suggested dry conditions. This period could correspond to the Medieval Warm Period (MWP) that is generally considered to be an episode of above average temperatures (Brázdil et al., 2005; Kaniewski et al., 2011). Transformation in clay minerals occurs during the later period of the Islamic period. Smectite was transformed into illite/smectite interstratified and chlorite into vermiculite. Colder conditions would have taken place during this critical period; at that time, pedogenesis was weak as shown by a decrease in the chlorite/smectite mixed layers. There was no major documented change in the settlements around the Amik Lake during this time (Eger, 2015). Thus, these clay mineralogical changes were mostly due to the climatic environmental change. During the Islamic period, there was no progressive climatic change, but a strong variability (Izdebski et al., 2016).

5.6. Ottoman age

Regarding to the human occupation, there was no change regarding the anthropic pressure on the environment except during the 19th century. The Amik Basin and its surrounding were weakly occupied and pastoralism was the dominant occupation (Gerritsen et al., 2008). Soil erosion was still occurring in the Amik Plain as attested by in our record by the occurrence of chlorite/

Please cite this article in press as: El Ouahabi, M., et al., Lacustrine clay mineral assemblages as a proxy for land-use and climate changes over the last 4 kyr: The Amik Lake case study, Southern Turkey, Quaternary International (2016), http://dx.doi.org/10.1016/j.quaint.2016.11.032

smectite mixed layers. The slight increase in the magnetic susceptibility during that period also suggests a detrital supply in the lake related to soil erosion (Fig. 6). This strong erosion was also associated with a high amount in the chlorite, which has not been significantly influenced by the pedogenic processes.

Changes in clay mineralogy would thus preferentially reflect climatic changes. Two different periods were identified: a warm one during the early time followed by a colder and drier climate. The warm and humid conditions are attested by rise in the smectite amount, Sm/Il ratio, Sm/(II + Ch) and Ka/(II + Ch). The following cold period is characterized by a fall in Sm/Il ratio and Sm/(II + Ch). This colder interval may correspond to the Little Ice Age (LIA) climatic event (Briffa, 2000; Jones et al., 2001; Osborn and Briffa, 2006; Richter et al., 2009).

The end of the Ottoman period is also marked by a marked increase in chlorite reaching more than 40% and the near disappearance of illite. The increase in chlorite associate with a small increase in magnetic susceptibility would be linked to renew erosion of the mountainous ranges surrounding the Amik Plain. At the end of the 19th century and at the beginning of the 20th century, the anthropic pressure increased again on the environment with the industrial development. In particular, the railway between Bagdad and Istanbul was constructed and its path goes through the catchment of the Afrin and the Karasu Rivers. An acute deforestation of the Amanus occurred close to the railroad to respond to the lack of coal during World War I (Huvelin, 1919).

5.7. Modern period

The Modern period is characterized by a renewed intensive agriculture surrounding Antioch (Antakya), which became a more important city. The present period is reminiscent of the Roman period with an engineered water drainage network in the Amik Plain and along the Karasu River that has driven an important agricultural development and a decrease in pastoralism. In particular, the grasslands on the ophiolites complex were converted to forests or arable lands (Gündoğan et al., 2011), croplands sharply increased and bareground decreased (Kilic et al., 2006). Marathianou et al. (2000) noted that in the Levsos Island, soils under pastures have the strong erosion among the various types of land use and this conversion is likely cause of soil erosion. Like during the Roman period, the modern period is characterized by a decrease/absence of chlorite as well as of mixed layers chlorite/smectite, which illustrates that a more intense agricultural

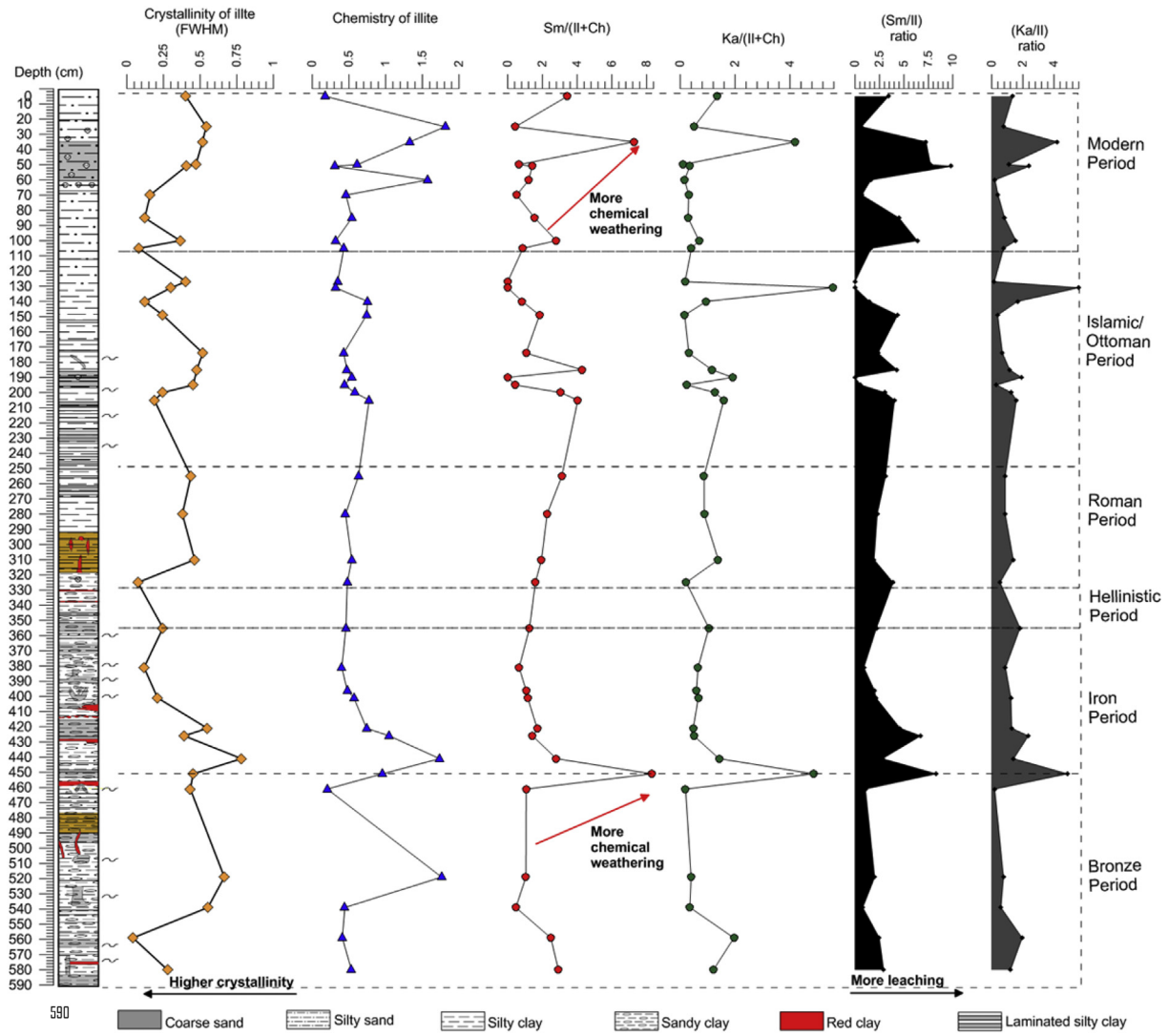

Fig. 6. Down core variations in crystallinity of illite (FWHM, values given in °2Theta Cu Kα), illite chemistry and various clay minerals as environmental proxies in the Amik Lake sediments. Sm/(Il + Ch), Ka/(Ii + Ch), (Sm/Ka) ratio and (Ka/Il) ratio evolution were used as climate proxy. Smectite (Sm), illite (Il), chlorite (Ch), kaolinite (Ka).

Please cite this article in press as: El Ouahabi, M., et al., Lacustrine clay mineral assemblages as a proxy for land-use and climate changes over the last 4 kyr: The Amik Lake case study, Southern Turkey, Quaternary International (2016), http://dx.doi.org/10.1016/j.quaint.2016.11.032

development is not always synonymous with large soil erosion if the sensitive areas are well managed.

Clay mineralogy during this period is also characterized by a significant increase in kaolinite, Sm/Il ratio, Sm/(Il + Ch) and Ka/(Il + Ch). A high chemistry of illite would be related to the current warm climate triggering an efficient hydrolysis. In addition, the appearance of illite/smectite mixed layers characterizing the actual soils are in agreement with the current warm climate and the intense land-use marked by the extension olives, grapevines, grain, and forest on the upland slopes (Casana, 2008).

Magnetic susceptibility and clay mineralogy in the Amik Lake sediment maintains climate shifts including many globally recognized events like the Medieval Warm Period (MWP) and Little Ice Age (LIA). This work represents the first extensive clay mineralogy and magnetic susceptibility study. The magnetic susceptibility fluctuations are related to grain-size and indicated the input of terrigenous material in the lake. The highest magnetic susceptibility values correspond to warm period with high chemical weathering. However, the lowest values provide cold conditions. This study confirms that the magnetic susceptibility signal in the Amik Lake is largely a proxy for climate change.

6. Conclusion

The Amik Lake sedimentary record typically resulted from the erosion of soils and weathered sediments developed in the watershed of the Amik Plain. Smectite, illite, kaolinite and chlorite/smectite mixed layers assemblages represented a detrital fraction of the sediments. The changes in their relative abundance, illite crystallinity and its chemistry thus reflect changes in the sources and modifications of the environmental conditions prevailing in the Amik watershed in relation with climatic changes and/or land-use.

The change in the crystallinity of illite and in the abundance of smectite, kaolinite, chlorite/smectite and illite/smectite were an indirect effect of pedogenesis and/or a weathering proxy. In addition anthropogenic modification in the watershed (e.g., water channelling) can indirectly change the clay source, affecting the composition of clay mineral assemblages.

The most intense erosion phase occurred during the Bronze/Iron Ages as indicated by the clay and magnetic susceptibility proxies. During the Roman period and until present days, less soil erosion showed due to much less intense settlement in the watershed of Amik Lake. As post-sedimentary conditions are marked in the Amik Lake deposits, clay mineral transformation were showed, especially during the Islamic/Ottoman period suggesting intense chemical weathering and pedogenesis transformations related to climate change.

Acknowledgment

This research was supported partially by the University of Liege and the EU in the context of the MSCA-COFUND-BeIPD project.

References

Ackermann, O., Greenbaum, N., Bruins, H., Porat, N., Bar-Matthews, M., Almogi-Labin, A., Schilman, B., Ayalon, A., Horwitz, L.K., Weiss, E., Maeir, A.M., 2014. Palaeoenvironment and anthropogenic activity in the southeastern Mediterranean since the mid-Holocene: the case of Tell es-Safi/Gath, Israel. Quat. Int. 328, 226–243.

Akyuz, H.S., Altunel, E., Karabacak, V., Yalciner, C.C., 2006. Historical earthquake activity of the northern part of the Dead sea Fault zone, Southern Turkey. Tectonophysics 426, 281–293.

Altunel, E., Meghraoui, M., Karabacak, V., Akyüz, S.H., Ferry, M., Yalçıner, Ç., Munschy, M., 2009. Archaeological sites (tell and road) offset by the dead Sea Fault in the Amik basin, southern Turkey. Geophys. J. Int. 179, 1313–1329.

Ambraseys, N., White, D., 1997. The seismicity of the eastern Mediterranean region 550-1 bc: a re-appraisal. J. Earthq. Eng. 1, 603–632.

Ambraseys, N.N., 1989. Temporary seismic quiescence: SE Turkey. Geophys. J. Int. 96, 311–331.

Appleby, P.G., 2002. Chronostratigraphic techniques in recent sediments. In: Tracking Environmental Change Using Lake Sediments. Springer, Netherlands, pp. 171–203.

Atalay, I., 1997. Red mediterranean soils in some karstic regions of Taurus Mountains, Turkey. Catena 28, 247–260.

Berglund, B.E., 2003. Human impact and climate changes—synchronous events and a causal link? Quat. Int. 105, 7–12.

Biscaye, P.E., 1965. Mineralogy and sedimentation of recent deep-sea clay in Atlantic Ocean and adjacent seas and oceans. Geol. Soc. Am. Bull. 76, 803–832.

Boulton, S.J., Robertson, A.H.F., Ellam, R.M., Safak, U., Unlügenc, U.C., 2007. Strontium isotopic and micropalaeontological dating used to help redefine the stratigraphy of the neotectonic Hatay Graben, Southern Turkey. Turkish J. Earth Sci. 16, 1–39.

Braidwood, R., Braidwood, L., 1960. Excavations in the Plain of Antioch I. In: AJ, P. (Ed.), The Earlier Assemblages, Chicago.

Brázdil, R., Pfister, C., Wanner, H., Von Storch, H., Luterbacher, J., 2005. Historical climatology in europe—the state of the art. Clim. Change 70, 363–430.

Briffa, K.R., 2000. Annual climate variability in the holocene: interpreting the message of ancient trees. Quat. Sci. Rev. 19, 87–105.

Buurman, P., Meijer, E., Van Wijck, J., 1988. Weathering of chlorite and vermiculite in ultramafic rocks of Cabo Ortegal, Northwestern Spain. Clays Clay Miner. 36, 263–269.

Çalışkan, V. (2008) Human-induced wetland degradation: a case study of Lake Amik (Southern Turkey). Pp. Third İnternational Conference on Water Observation and Information System for Decision Support, Ohrid, Macedonia.

Capper, M.M., 2012. Urban Subsistence in the Bronze and Iron Ages: the Palaeoethnobotany of Tell Tayinat, Turkey. Environment: Department of Archaeology.

Casana, J., 2007. Structural transformations in settlement systems of the Northern Levant. Am. J. Archaeol. 111, 195–221.

Casana, J., 2008. Mediterranean valleys revisited: linking soil erosion, land use and climate variability in the Northern Levant. Geomorphology 101, 429–442.

Casana, J., 2009. Alalakh and the archaeological landscape of Mukish: the political geography and population of a Late Bronze age kingdom. Bull. Am. Sch. Orient. Res. 7–37.

Casana, J., 2012. 7 settlement, territory, and the political landscape of Late Bronze Age polities in the Northern Levant. Archeol. Pap. Am. Anthropol. Assoc. 22, 107–125.

Casana, 2014. The late roman landscape of the northern levant: a view from Tell Qarqur and the lower Orontes River Valley. Oxf. J. Archaeol. 33, 193–219.

Chamley, H., 1989. Clay Sedimentology. Springer-Verlag, p. 623.

Chipera, S.J., Bish, D.L., 2001. Baseline studies of the clay minerals society source clays: powder x-ray diffraction analyses. Clays Clay Miner. 49, 398–409.

Costantini, E.A., Bucelli, P., Priori, S., 2012. Quaternary landscape history determines the soil functional characters of terroir. Quat. Int. 265, 63–73.

De Visser, J., Chamley, H., 1990. Clay Mineralogy of the Pliocene and Pleistocene of Hole 653a, Western Tyrrhenian Sea (odp leg 107).

Dodson, J.R., Taylor, D., Ono, Y., Wang, P., 2004. Climate, human, and natural systems of the PEP II transect. Quat. Int. 118, 3–12.

Dotterweich, M., 2008. The history of soil erosion and fluvial deposits in small catchments of central Europe: deciphering the long-term interaction between humans and the environment — a review. Geomorphology 101, 192–208.

Drake, B.L., 2012. The influence of climatic change on the late Bronze age collapse and the Greek Dark ages. J. Archaeol. Sci. 39, 1862–1870.

Edwards, K.J., Whittington, G., 2001. Lake sediments, erosion and landscape change during the Holocene in Britain and Ireland. Catena 42, 143–173.

Eger, A.A., 2011. The swamps of home: marsh formation and settlement in the Early Medieval Near East. J. Near East. Stud. 70, 55–79.

Eger, A.A., 2015. The Islamic-byzantine Frontier: Interaction and Exchange Among Muslim and Christian Communities. IB Tauris.

El Albani, A., Meunier, A., Macchiarelli, R., Ploquin, F., Tournepiche, J.F., 2011. Local environmental changes recorded by clay minerals in a karst deposit during MIS 3 (La Chauverie, SW France). Quat. Int. 241, 26–34.

Esquevin, J., 1969. Influence de la composition chimique des illites sur leur cristallinité. Bull. Cent. Rech. Pau-SNPA 3, 147–153.

Fagel, N., Boski, T., Likhoshway, L., Oberhaensli, H., 2003. Late quaternary clay mineral record in central lake Baikal (Academician ridge, Siberia). Palaeogeogr. Palaeoclimatol. Palaeoecol. 193, 159–179.

Ferrage, E., Lanson, B., Sakharov, B.A., Geoffroy, N., Jacquot, E., Drits, V.A., 2007. Investigation of dioctahedral smectite hydration properties by modeling of x-ray diffraction profiles: influence of layer charge and charge location. Am. Mineral. 92, 1731–1743.

Friedman, I., Trembour, F.W., Hughes, R.E., 1997. Obsidian hydration dating, in chronometric dating in archaeology. In: Taylor, R.E., Aitken, M.J. (Eds.), Advances in Archaeological and Museum Science, vol. 2. Springer/Plenum Press, New York, pp. 297–321.

Gerritsen, F., De Giorgi, A., Eger, A., Özbal, R., Vorderstrasse, T., 2008. Settlement and landscape transformations in the Amuq Valley, Hatay: a long-term perspective. Anatolica 34, 241–314.

Gingele, F.X., 1996. Holocene climatic optimum in southwest Africa - evidence from the marine clay mineral record. Palaeogeogr. Palaeoclimatol. Palaeoecol. 122, 77–87.

Guidoboni, E., Comastri, A., Traina, G., 1994. Catalogue of Ancient Earthquakes in the Mediterranean Area up to the 10th Century. SGA.
Gülen, L., Barka, A., Toksöz, M.N., 1987. Continental collision and related complex deformation: Maras triple junction and surrounding structures, SE Turkey. Hacettepe Univ. Earth Sci. J. 14, 319–336.
Gün, M., Erdem, A., 2003. Agricultural master plan of Hatay. Ministry of Agriculture and Rural Affairs-Agricultural Directorate of Hatay (in Turkish).
Gündoğan, R., Özyurt, H., Akay, A., 2011. The effects of land use on properties of soils developed over ophiolites in Turkey. Int. J. For. Soil Eros. (IJFSE) 1, 36–42.
Günster, N., Skowronek, A., 2001. Sediment–soil sequences in the Granada Basin as evidence for long-and short-term climatic changes during the Pliocene and Quaternary in the Western Mediterranean. Quat. Int. 78, 17–32.
Haldon, J., Roberts, N., Izdebski, A., Fleitmann, D., McCormick, M., Cassis, M., Doonan, O., Eastwood, W., Elton, H., Ladstätter, S., Manning, S., Newhard, J., Nicoll, K., Telelis, I., Xoplaki, E., 2014. The climate and environment of Byzantine Anatolia: Integrating science, history, and archaeology. J. Interdiscip. Hist. 45, 113–161.
Harp, E.L., Jibson, R.W., 1996. Landslides triggered by the 1994 northridge, California, earthquake. Bull. Seismol. Soc. Am. 86, S319–S332.
Hovius, N., Meunier, P., Lin, C.-W., Chen, H., Chen, Y.-G., Dadson, S., Horng, M.-J., Lines, M., 2011. Prolonged seismically induced erosion and the mass balance of a large earthquake. Earth Planet. Sci. Lett. 304, 347–355.
Hubert-Ferrari, A., Avsar, U., El Ouahabi, M., Lepoint, G., Martinez, P., Fagel, N., 2012. Paleoseismic record obtained by coring a sag-pond along the north Anatolian fault (Turkey). Ann. Geophys. 55, 929–953.
Hubert, F., Caner, L., Meunier, A., Lanson, B., 2009. Advances in characterization of soil clay mineralogy using x-ray diffraction: from decomposition to profile fitting. Eur. J. Soil Sci. 60, 1093–1105.
Huvelin, P., 1919. Que vaut la syrie? Librairie ancienne Honoré Champion.
Inoue, A., Bouchet, A., Velde, B., Meunier, A., 1989. Convenient technique for estimating smectite layer percentage in randomly interstratified illite/smectite minerals. Clays Clay Miner. 37, 227–234.
Izdebski, A., Pickett, J., Roberts, N., Waliszewski, T., 2016. The environmental, archaeological and historical evidence for regional climatic changes and their societal impacts in the eastern mediterranean in late antiquity. Quat. Sci. Rev. 136, 189–208.
Jalut, G., Dedoubat, J.J., Fontugne, M., Otto, T., 2009. Holocene circum-Mediterranean vegetation changes: climate forcing and human impact. Quat. Int. 200, 4–18.
Jones, P., Osborn, T., Briffa, K., 2001. The evolution of climate over the last millennium. Science 292, 662–667.
Kaniewski, D., Paulissen, E., Van Campo, E., Weiss, H., Otto, T., Bretschneider, J., Van Lerberghe, K., 2010. Late second–early first millennium bc abrupt climate changes in coastal Syria and their possible significance for the history of the eastern mediterranean. Quat. Res. 74, 207–215.
Kaniewski, D., Van Campo, E., Paulissen, E., Weiss, H., Bakker, J., Rossignol, I., Van Lerberghe, K., 2011. The medieval climate anomaly and the Little Ice Age in coastal Syria inferred from pollen-derived palaeoclimatic patterns. Glob. Planet. Change 78, 178–187.
Kaptijn, E., Poblome, J., Vanhaverbeke, H., Bakker, J., Waelkens, M., 2013. Societal changes in the Hellenistic, Roman and Early Byzantine periods. Results from the sagalassos territorial archaeological survey 2008 (Southwest Turkey). Anatol. Stud. 63, 75.
Karabacak, V., Altunel, E., 2013. Evolution of the northern dead sea fault zone in Southern Turkey. J. Geodyn. 65, 282–291.
Karabacak, V., Altunel, E., Meghraoui, M., Akyüz, H., 2010. Field evidences from northern dead sea fault zone (South Turkey): new findings for the initiation age and slip rate. Tectonophysics 480, 172–182.
Kübler, B., Jaboyedoff, M., 2000. Illite crystallinity. Comptes Rendus de l'Académie des Sciences-Series IIA-Earth Planet. Sci. 331 (2), 75–89.
Kilic, S., Evrendilek, F., Berberoglu, S., Demirkesen, A., 2006. Environmental monitoring of land-use and land-cover changes in a mediterranean region of Turkey. Environ. Monit. Assess. 114, 157–168.
Lanson, B., 1997. Decomposition of experimental x-ray diffraction patterns (profile fitting): a convenient way to study clay minerals. Clays Clay Miner. 45, 132–146.
Lanson, B., Besson, G., 1992. Characterization of the end of smectite-to-illite transformation: decomposition of x-ray patterns. Clays Clay Miner. 40, 40–52.
Lawrence, D., Philip, G., Wilkinson, K., Buylaert, J.P., Murray, A.S., Thompson, W., Wilkinson, T.J., 2015. Regional power and local ecologies: accumulated population trends and human impacts in the northern Fertile Crescent. Quat. Int. (in press).
Lehner, B., Verdin, K., Jarvis, A., 2008. New global hydrography derived from Spaceborne elevation data. Eos 89, 93–94.
Liebeschuetz, J.H.W.G., 1972. Antioch: City and Imperial Administration in the Later Roman Empire. Oxford University Press, USA.
Lombard, M., 1959. Un problème cartographié: Le bois dans la méditerranée musulmane (VIIE-XIE siècles. In: Proceedings of the Annales. Histoire, Sciences Sociales. JSTOR, pp. 234–254.
Lucke, B., Schmidt, M., Al-Saad, Z., Bens, O., Hüttl, R.F., 2005. The abandonment of the Decapolis region in Northern Jordan-forced by environmental change? Quat. Int. 135, 65–81.
Marathianou, M., Kosmas, C., Gerontidis, S., Detsis, V., 2000. Land-use evolution and degradation in lesvos (Greece): a historical approach. Land Degrad. Dev. 11, 63–73.
Marco, S., 2008. Recognition of earthquake-related damage in archaeological sites: examples from the dead sea fault zone. Tectonophysics 453, 148–156.
Marriner, N., Goiran, J.-P., Geyer, B., Matoïan, V., al-Maqdissi, M., Leconte, M., Carbonel, P., 2012. Ancient harbors and holocene morphogenesis of the ras Iibn Hani Peninsula (Syria). Quat. Res. 78, 35–49.
McCormick, M., Büntgen, U., Cane, M.A., Cook, E.R., Harper, K., Huybers, P., Litt, T., Manning, S.W., Mayewski, P.A., More, A.F., Nicolussi, K., 2012. Climate change during and after the Roman Empire: reconstructing the past from scientific and historical evidence. J. Interdiscip. Hist. 43 (2), 169–220.
Meadows, J., 2005. The Younger Dryas episode and the radiocarbon chronologies of the lake Huleh and Ghab valley pollen diagrams, Israel and Syria. Holocene 15, 631–636.
Moore, D.M., Reynolds, R.C., 1997. X-ray Diffraction and the Identification and Analysis of Clay Minerals. Oxford University Press, Oxford.
Moss, A.J., Walker, P.H., 1978. Particle transport by continental water flows in relation to erosion, deposition, soils, and human activities. Sediment. Geol. 20, 81–139.
Osborn, T.J., Briffa, K.R., 2006. The spatial extent of 20th-century warmth in the context of the past 1200 years. Science 311, 841–844.
Özşahin, E., Uygur, V., 2014. The effects of land use and land cover changes (LULCC) in Kuseyr Plateau of Turkey on erosion. Turkish J. Agric. For. 38 (4), 478–487.
Pandarinath, K., 2009. Clay minerals in SW Indian continental shelf sediment cores as indicators of provenance and palaeomonsoonal conditions: a statistical approach. Int. Geol. Rev. 51, 145–165.
Parlak, O., Rızaoğlu, T., Bağcı, U., Karaoğlan, F., Höck, V., 2009. Tectonic significance of the geochemistry and petrology of ophiolites in southeast Anatolia, Turkey. Tectonophysics 473, 173–187.
Pelle, T., Fabio, S., Gaetano Di, P., Allevato, E., Marino, D., Robustelli, G., Mauro, F., Russa, La, Pulice, L., 2013. Multidisciplinary study of Holocene archaeological soils in an upland Mediterranean site: natural versus anthropogenic environmental changes at Cecita Lake, Calabria, Italy. Quat. Int. 303, 163–179.
Pécsi, M., 1990. Loess is not just the accumulation of dust. Quat. Int. 7, 1–21.
Prichard, H.M., 1979. A petrographie study of the process of serpentinisation in ophiolites and the ocean crust. Contrib. Mineral. Petrol. 68, 231–241.
Renac, C., Meunier, A., 1995. Reconstruction (hipalaeothermal, conditons in a passive margin using illite-smectite mixed-layer series (bal scientific deep drill-hole, Ardeche, France). Clay Miner. 30, 107–118.
Reynolds, R., 1988. Mixed layer chlorite minerals. Rev. Mineral. Geochem. 19, 601–629.
Richter, T., Peeters, F., Van Weering, T., 2009. Late holocene (0–2.4 kabp) surface water temperature and salinity variability, Feni Drift, NE Atlantic Ocean. Quat. Sci. Rev. 28, 1941–1955.
Righi, D., Petit, S., Bouchet, A., 1993. Characterization of hydroxy-interlayered vermiculite and illite/smectite interstratified minerals from the weathering of chlorite in a cryorthod. Clays Clay Miner. 41, 484–484.
Righi, D., Velde, B., Meunier, A., 1995. Clay stability in clay-dominated soil systems. Clay Miner. 30, 45–54.
Robertson, A.H.F., 2002. Overview of the genesis and emplacement of mesozoic ophiolites in the eastern Mediterranean Tethyan region. Lithos 65, 1–67.
Schmidt, S., Howa, H., Mouret, A., Lombard, F., Anschutz, P., Labeyrie, L., 2009. Particle fluxes and recent sediment accumulation on the Aquitanian margin of Bay of Biscay. Cont. Shelf Res. 29, 1044–1052.
Sauer, D., Amit, R., Carnicelli, S., Costantini, E.A., 2015. Rates of soil forming processes and the role of aeolian influx. Quat. Int. 376, 1–4.
Singer, A., 1984. The paleoclimatic interpretation of clay minerals in sediments - a review. Earth Sci. Rev. 21, 251–293.
Thorez, J., 1976. Practical Identification of Clay Minerals. G. Lelotte, Liège, p. 90.
Tsatskin, A., Zaidner, Y., 2014. Geoarchaeological context of the later phases of mousterian occupation (80–115 ka) at Nesher Ramla, Israel: soil erosion, deposition and pedogenic processes. Quat. Int. 331, 103–114.
Varga, A., Újvári, G., Raucsik, B., 2011. Tectonic versus climatic control on the evolution of a loess–paleosol sequence at Beremend, Hungary: an integrated approach based on paleoecological, clay mineralogical, and geochemical data. Quat. Int. 240, 71–86.
Velde, B., Meunier, A., 2008. The Origin of Clay Minerals in Soils and Weathered Rocks, p. 406. Heidelberg.
Vogel, S., Märker, M., Rellini, I., Hoelzmann, P., Wulf, S., Robinson, M., Steinhübelh, L., Di Maioi, G., Imperatorej, C., Kastenmeierj, P., Liebmannf, L., Espositoj, D., Seilerj, F., 2016. From a stratigraphic sequence to a landscape evolution model: late Pleistocene and Holocene volcanism, soil formation and land use in the shade of Mount Vesuvius (Italy). Quat. Int. 394, 155–179.
Weaver, C., 1989. Clays, Muds, and Shales (Developments in Sedimentology).
Weiss, B., 1982. The decline of Late Bronze Age civilization as a possible response to climatic change. Clim. Change 4, 173–198.
Wilkinson, T.J., 1997. The history of the lake of Antioch: a preliminary note. In: Young, G., Chavalas, M., Averback, R. (Eds.), Rossing Boundaries and Linking Horizons: Studies in Honor of Michael c. Astour on His 80th Birthday. CLD Press, Bethesda, Maryland.
Wilkinson, T.J., 1999. Holocene valley fills of southern Turkey and northwestern Syria: recent geoarchaeological contributions. Quat. Sci. Rev. 18, 555–571.
Wilkinson, T.J., 2000. Geoarchaeology of the Amuq plain. In: Yener, A., Edens, C., Harrison, T., Verstraete, J., Wilkinson, T.J. (Eds.), The Amuq Valley Regional Project, 1995–1998, vol. 104, pp. 163–220. American Journal of Archaeology.
Wilkinson, T.J., Friedman, E.S., Alp, E., Stampfl, A.P.J., 2001. The geoarchaeology of a lake basin: spatial and chronological patterning of sedimentation in the Amuq Plain, Turkey. J. Name Recherches Archeometriques 211–226.

Please cite this article in press as: El Ouahabi, M., et al., Lacustrine clay mineral assemblages as a proxy for land-use and climate changes over the last 4 kyr: The Amik Lake case study, Southern Turkey, Quaternary International (2016), http://dx.doi.org/10.1016/j.quaint.2016.11.032

Wilkinson, T.J., Rayne, L., 2010. Hydraulic landscapes and imperial power in the near east. Water Hist. 2, 115–144.
Yener, K., Yener, K., 2005. Alalakh spatial organization. Amuq Val. Regonal Proj. 1, 1995–2002.
Yener, K.A., Batiuk, S., 2010. Tell Atchana, Ancient Alalakh: the 2003–2004 Excavation Seasons/ed. By Kutlu Aslihan Yener. With contrib. By Stephen Batiuk [ua]. Ege Yayınları.
Yener, K.A., Edens, C., Harrison, T.P., Verstraete, J., Wilkinson, T.J., 2000. The Amuq Valley regional project, 1995-1998. Am. J. Archaeol. 104, 163–220.
Zielhofer, C., Faust, D., Linstädter, J., 2008. Late Pleistocene and Holocene alluvial archives in the Southwestern Mediterranean: changes in fluvial dynamics and past human response. Quat. Int. 181, 39–54.

Please cite this article in press as: El Ouahabi, M., et al., Lacustrine clay mineral assemblages as a proxy for land-use and climate changes over the last 4 kyr: The Amik Lake case study, Southern Turkey, Quaternary International (2016), http://dx.doi.org/10.1016/j.quaint.2016.11.032